doi:10.1246/cl.2012.874
874 Published on the web August 11, 2012

Histone-like Protein HCcp3-induced Liquid Crystalline DNA Condensation

Shiyong Sun,*[1] Joseph T. Y. Wong,[2] Faqin Dong,[1] and Mingxue Liu[3]
[1]*Key Laboratory of Solid Waste Treatment and Resource Recycle, School of Environment and Resource, Southwest University of Science and Technology, Mianyang, Sichuan 621010, P. R. China*
[2]*Division of Life Sciences, Hong Kong University of Science and Technology, Clear Water Bay, Kowloon, Hong Kong SAR 00852, P. R. China*
[3]*School of Life Science and Engineering, Southwest University of Science and Technology, Mianyang, Sichuan 621010, P. R. China*

(Received May 18, 2012; CL-120431; E-mail: shysun@swust.edu.cn)

From prokaryotes to eukaryotes, the DNA condensation process by basic proteins is essential to store the genome in vivo. The surface charge inversion with a DNA/HCcp3 charge ratio of 0.7/1 indicates a role for HCcp3-mediated counter ion-driven mechanism in DNA condensation. The formation of the cholesteric liquid-crystalline phase of DNA–HCcp3 complexes occurred when DNA charges were neutralized. The results suggest that DNA condensation processes by HCcp3 can be divided into two distinctive binding stages: the first state, prior to condensation, involves an entropy-driven binding process of HCcp3 to the DNA, while the second state is an electrostatically driven condensing and assembling process.

DNA condensation is a macroscopic phase separation process in which a dense phase of aggregated DNA separates from a phase of poor DNA.[1] Cationic counter ions are well known to tightly compact DNA into multiple condensation states.[2] These condensing agents include multivalent cations of hexaammine cobalt,[3,4] spermidine,[5] and spermine,[6] as well as protamines,[1] histones,[7] and histone-like proteins (HLPs)[8] that are strong positively charged basic DNA-binding proteins. The counter ion-mediated DNA condensation process, which is referred to as the compensation of the negatively charged DNA by strong attraction of cationic counter ions, is responsible for some of the physical properties and biological function in biocolloidal systems.[2] Polyamine and RecA protein have been shown to organize DNA into liquid-crystalline phases.[9,10]

Histoneless dinoflagellate chromosomes are permanently condensed in the liquid-crystalline (LC) state throughout the cell cycle. It seems that cholesteric LC DNA organization is required for dinoflagellates stabilizing their genomes without nucleosome.[11] Four HLPs isoforms from the dinoflagellate Crypthecodinium cohnii (HCcp) were previously identified and denoted as HCcp1–HCcp4.[12] Sequence-based primary structure analysis of the recombinant form of HCcp3 suggests that it contains a total of 125 amino acid residues, wherein the C-terminal region contains 27 positively charged residues (Arg + Lys), and the N-terminal region contains 7 negatively charged residues (Asp + Glu). Therefore, the integrated positive charges are equal to $+20e$ (e, elemental charge). Even though previous study suggested that HCcp3 is an efficient DNA-binding and condensing protein, little is known about their macroscopic condensation phases.[13]

The DNA fragments encoding HCcp3 (GenBank accession: AY128510.1) were amplified by PCR. The PCR product was cloned into the expression vector pQE30 (Qiagen Corporation, Valencia, CA, USA). The recombinant HCcp3 was overexpressed by using QIA expressionist protein expression system (Qiagen Corporation) and purified under the denatured condition. The recombinant HCcp3 was further purified by Bio-scale Mini UNOsphere S cartridge using Biological LPC (Bio-Rad). Salmon sperm DNA used in this study was purchased from Sigma-Aldrich. The sheared thread-like DNA was fragmented (less than 1500 bp) by sonication. The details of experimental materials and methods can be found in the Supporting Information (SI).[17]

To determine the changes in DNA charge characteristics upon DNA binding, electrophoretic mobility shift assay (EMSA) was used to detect the electrophoretic shift of DNA–HCcp3 interactions at different concentration ratios (DNA/HCcp3 charge ratio express as simply anion/cation ratio throughout this paper). The free DNAs showed no band shifts at low HCcp3 concentration (Figure 1). With increasing HCcp3 levels, however, DNA–HCcp3 complexes formed, causing the DNA bands to significantly shift starting from the 16/1 charge ratio and the DNA–HCcp3 complexes were predominantly in the aggregated form around the 1/1 charge ratio (Figure 1A). At high HCcp3 concentrations (charge ratio $<0.5/1$), the retarded DNA–HCcp3 complex bands significantly shifted direction toward the oppositely charged pole as a result of surface charge inversion, suggesting that the excess HCcp3 in the well bound to the surface of DNA–HCcp3 complexes and overcompensated for the DNA charges.

The dynamic electrophoretic mobility (EPM) of DNA–HCcp3 complexes was quantitatively analyzed by Zeta-PALS, a highly sensitive technique for measuring low mobility shifts. As HCcp3 concentration increased, the EPM value of DNA–HCcp3 complexes changed from negative to positive with a threshold charge ratio of 0.7/1 (Figure 1B). This Zeta-PALS-determined surface charge inversion threshold is comparable to the EMSA result that yielded a charge ratio of 0.5/1. Since the Zeta-PALS-determined surface charge inversion threshold analysis was conducted under the same buffer conditions and without the Ethidium bromide staining step, the critical point of surface charge inversion is likely more reliable than the EMSA-determined threshold. Taken together, the results of electrophoretic mobility assays suggest that the closeness achieved by HCcp3-mediated DNA condensation may occur by counter ion attraction.

Isothermal titration microcalorimetry (ITC) was used to detect the changes associated with the thermodynamic titration of HCcp3-mediated DNA condensation after adding HCcp3 to DNA and, conversely, DNA to HCcp3 (Figure 2). The ITC

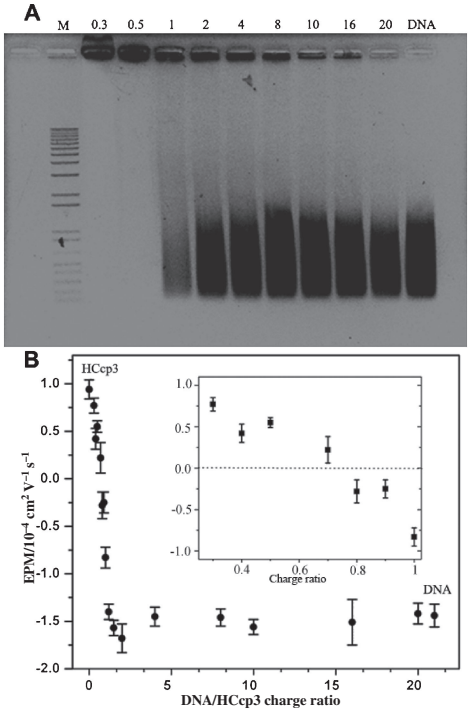

Figure 1. Electrophoretic mobility assays demonstrating the HCcp3-mediated surface charge inversion of DNA. (A) EMSA in the presence of HCcp3 with various charge ratios. (B) Quantitative DNA–HCcp3 electrophoretic mobility was measured by Zeta-PALS with different charge ratios. Inset in (B): the surface charge inversion region of DNA–HCcp3. The DNA concentration used in (A), (B) is 0.1 mg mL^{-1}.

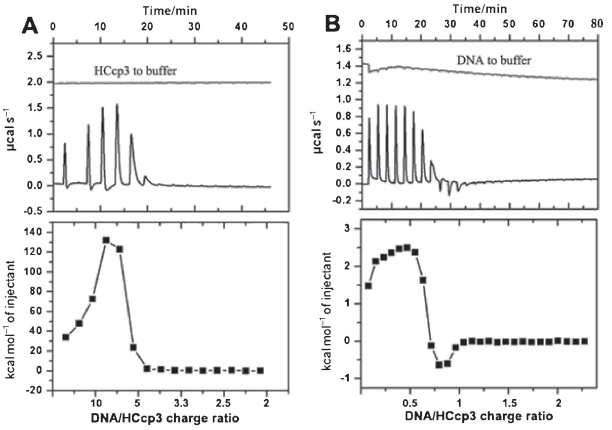

Figure 2. The isothermal titration microcalorimetry measurement between HCcp3 and DNA. (A) HCcp3 in the syringe was injected to DNA in the cell. (B) DNA in the syringe was injected to HCcp3 in the cell. (A) DNA 64 μg mL^{-1}, HCcp3 0.58 mg mL^{-1}. (B) DNA 0.75 mg mL^{-1}, HCcp3 0.14 mg mL^{-1}.

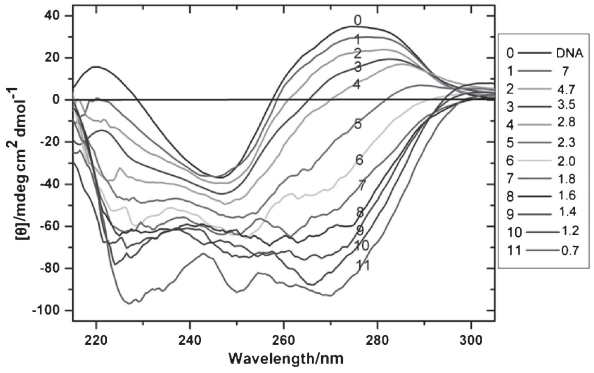

Figure 3. The circular dichroism spectra of 0.58 mg mL^{-1} HCcp3 titrated into 0.1 mg mL^{-1} DNA. The DNA/HCcp3 charge ratio of every titration reaction is indicated in the image. Curve 10 shows the characteristic band of cholesteric LC phase formation near 265 nm.

profiles shown in Figures 2A and 2B are quite different and may be caused by the discrepancy of binding environments between HCcp3 to DNA and DNA to HCcp3. The integrated ITC curves show that the binding reaction of HCcp3 to DNA is endothermic in two stages (Figure 2A), which suggested that this reaction may be an entropy-driven process, with a net increase in entropy.[14] The heat generated by the initial binding stage gradually increased and reached a maximum value when the completion of the initial binding stage occurred at a charge ratio of 8/1. Following the first binding stage, the second binding stage occurred after further addition of HCcp3. As the binding sites become occupied, the magnitude of the heat generated per injection decreased until all the binding sites were saturated. The completion of the second stage occurred at a charge ratio of 4/1. Interestingly, the titration patterns of adding DNA to HCcp3 were quite different from those of adding HCcp3 to DNA (Figure 2B): the addition of DNA to HCcp3 showed an endothermic reaction in the initial binding stage, similar to adding HCcp3 to DNA. However, an exothermal stage involving a small exothermal enthalpy change followed, which continued upon further addition of DNA. The maximum negative enthalpy may be due to charge neutralization (Figure 2B).

As shown in Figure 3, the initial B-type DNA molar ellipticity was significantly changed in the positive bands at 275 and 220 nm in the presence of HCcp3. In previous studies, the formation of the homogenous cholesteric LC DNA conformation exhibits a negatively enhanced circular dichroism (CD) spectrum from 265 to 270 nm that is associated with B-Ψ (PSI) transition.[15] In our study, the observed CD spectra displayed an intense negative peak at near 265 nm with charge ratio of 1.2/1, therefore, indicating that a cholesteric LC phase had been formed (Figure 3).

The fraction containing aggregated DNA–HCcp3 complexes was separated from the supernatant by centrifugation, which forced dense packing of the precipitate. The collected pellets were deposited between a glass slide and a coverslip for observation by polarizing microscopy (PM). The aggregated DNA–HCcp3 pellets with charge ratios ranging from 12/1 to 1/1 presented multiple cholesteric LC textures (Figure 4). The typical fingerprint patterns were formed with DNA/HCcp3 ratios of 12/1 and 7/1 (Figures 4A and 4B). PM and AFM images show that DNA–HCcp3 (charge ratio of 1/1) pellets exhibited an ordered, bundle-like LC texture in the absence of fingerprint patterns (Figures 4C and 4D). In the cholesteric LC phase, the DNA molecules are aligned in parallel layers and are continuously oriented along a cholesteric axis that display the

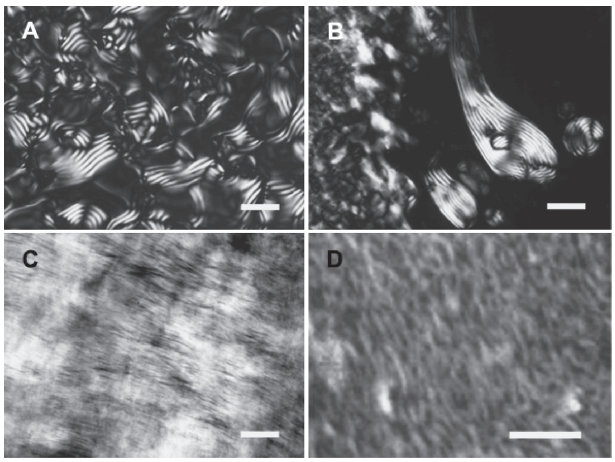

Figure 4. Various DNA–HCcp3 textures observed by microscopy. (A)–(C) Pellets collected by centrifugation were observed under a polarizing microscope. (D) The droplet containing DNA–HCcp3 complexes was observed by an atomic force microscope. The DNA/HCcp3 charge ratios of (A) to (D) are 12/1, 7/1, 1/1, and 1/1, respectively. Scale bars: (A) to (C) 20 μm and (D) 250 nm.

classical fingerprint patterns if the helical pitch is longer than the resolution limit (about 250 nm) of optical microscopy.[15] As described for the CD measurement experiments, the cholesteric LC phase formed in the region where DNA charges are neutralized (Figure 3). Therefore, we can reasonably infer that HCcp3 compacted DNA (charge ratio of 1/1) into a dense cholesteric phase with a helical pitch beyond PM observation.

The multiple independent techniques performed in this study give consistent results for the DNA and HCcp3 interaction characteristics in the same buffer conditions. The CD spectra and microscopy observations described here suggest that HCcp3 is not only an efficient DNA condensing agent, similar to universal basic proteins but also can help in spatially assembling DNA into the cholesteric LC phase (Figures 3 and 4). This is an interesting result when compared to other basic proteins, such as HU,[8] H1,[16] and protamines,[1] since DNA condensation by these basic proteins cannot form the LC phases in vitro, to the best of our knowledge.

The surface charge inversion of DNA by HCcp3 binding was observed in our electrophoretic mobility assays (Figure 1), indicating a role for electrostatic interactions in HCcp3-mediated DNA condensation. We previously demonstrated that the orderly LC DNA–HCcp3 texture cannot form at very diluted DNA concentrations.[13] This suggests that a crowded macromolecular environment may be necessary to promote the electrostatic attractions that form the intermolecular bundle-like DNA–HCcp3 complexes, since the densely packed environment might be able to overcome the entropy barrier in order to achieve the more stable cholesteric LC state.[11] The previously published ITC results from entropy-driven DNA condensation demonstrated a similar endothermic two-stage condensation process with small positive binding enthalpies.[14] According to this entropy-driven binding model, DNA condensation by HCcp3 was expected not to demonstrate an exothermic stage.

Based on the presented results, the sequential DNA condensation stages mediated by HCcp3 are the following two stages. (a) Prior to condensation, the DNA–HCcp3 complex formation process is a counter ionic attraction by positively charged HCcp3 bound on the surface of negatively charged DNA. (b) This is followed by a DNA condensation self-assembly resulting from DNA charge neutralization by the binding of an adequate level of HCcp3. During the initial binding stage (a), HCcp3 bound to DNA with a charge ratio beyond the threshold concentration for charge neutralization. In the (b) binding stage, however, the neutralized DNA fraction increases and reaches a threshold concentration high enough to mediate the electrostatic mechanism that governs HCcp3-mediated DNA condensation, leading to the formation of the cholesteric LC DNA organization.

In conclusion, our results consistently demonstrated that HCcp3 is an efficient DNA condensing and assembling protein. The surface charge inversion occurred with a charge ratio at 0.7/1, indirectly suggesting that the electrostatic interaction role of HCcp3-induced LC DNA condensation. The results of the dynamic CD and ITC titration experiments suggested that the homogenous cholesteric LC phase formed while HCcp3 neutralized the DNA charges at a charge ratio of approximately 1/1. The results implicate a possible significant dual role for HCcp3 in DNA charge neutralization and in organizing the cholesteric liquid-crystalline phase DNA in vivo.

The present work was partly supported by RPC 06/07 SC10 and National Natural Science Foundation of China (Nos. 41102213 and 41130746).

References and Notes

1 A. C. Toma, M. de Frutos, F. Livolant, E. Raspaud, *Biomacromolecules* **2009**, *10*, 2129.
2 B. A. Todd, D. C. Rau, *Nucleic Acids Res.* **2008**, *36*, 501.
3 D. Matulis, I. Rouzina, V. A. Bloomfield, *J. Mol. Biol.* **2000**, *296*, 1053.
4 B. I. Kankia, V. Buckin, V. A. Bloomfield, *Nucleic Acids Res.* **2001**, *29*, 2795.
5 Z. Lin, C. Wang, X. Feng, M. Liu, J. Li, C. Bai, *Nucleic Acids Res.* **1998**, *26*, 3228.
6 J. DeRouchey, R. R. Netz, J. O. Rädler, *Eur. Phys. J. E: Soft Matter Biol. Phys.* **2005**, *16*, 17.
7 E. Raspaud, J. Pelta, M. de Frutos, F. Livolant, *Phys. Rev. Lett.* **2006**, *97*, 068103.
8 T. Sarkar, I. Vitoc, I. Mukerji, N. V. Hud, *Nucleic Acids Res.* **2007**, *35*, 951.
9 K. Okoshi, T. Nishinaka, Y. Doi, R. Hara, M. Hashimoto, E. Yashima, *Chem. Commun.* **2007**, 2022.
10 M. Saminathan, T. Thomas, A. Shirahata, C. K. S. Pillai, T. J. Thomas, *Nucleic Acids Res.* **2002**, *30*, 3722.
11 A. Minsky, R. Ghirlando, Z. Reich, *J. Theor. Biol.* **1997**, *188*, 379.
12 J. T. Y. Wong, D. C. New, J. C. W. Wong, V. K. L. Hung, *Eukaryotic Cell* **2003**, *2*, 646.
13 Y.-H. Chan, J. T. Y. Wong, *Nucleic Acids Res.* **2007**, *35*, 2573.
14 W. Kim, Y. Yamasaki, W.-D. Jang, K. Kataoka, *Biomacromolecules* **2010**, *11*, 1180.
15 F. Livolant, A. Leforestier, *Prog. Polym. Sci.* **1996**, *21*, 1115.
16 R. Sarkar, S. K. Pal, *Biomacromolecules* **2007**, *8*, 3332.
17 Supporting Information is also available electronically on the CSJ-Journal Web site, http://www.csj.jp/journals/chem-lett/index.html.

